THE UNIVERSITY of EDINBURGH

Edinburgh Research Explorer

A comparative prospective life cycle assessment of coal-fired power plants in the US with MEA/MOF-based carbon capture

Citation for published version:
Tao, Y & Brander, M 2024, 'A comparative prospective life cycle assessment of coal-fired power plants in the US with MEA/MOF-based carbon capture', *Journal of Cleaner Production*, vol. 456, 142418, pp. 1-11. https://doi.org/10.1016/j.jclepro.2024.142418

Digital Object Identifier (DOI):
10.1016/j.jclepro.2024.142418

Link:
Link to publication record in Edinburgh Research Explorer

Document Version:
Peer reviewed version

Published In:
Journal of Cleaner Production

General rights
Copyright for the publications made accessible via the Edinburgh Research Explorer is retained by the author(s) and / or other copyright owners and it is a condition of accessing these publications that users recognise and abide by the legal requirements associated with these rights.

Take down policy
The University of Edinburgh has made every reasonable effort to ensure that Edinburgh Research Explorer content complies with UK legislation. If you believe that the public display of this file breaches copyright please contact openaccess@ed.ac.uk providing details, and we will remove access to the work immediately and investigate your claim.

Download date: 17. Mar. 2025

A Comparative Prospective Life Cycle Assessment of Coal-Fired Power Plants in the US with MEA/MOF-Based Carbon Capture

Yiran Tao [a, b, *], Matthew Brander [b]

[a] China-UK Low Carbon College, Shanghai Jiao Tong University, Shanghai 200240, China

[b] University of Edinburgh Business School, 29 Buccleuch Place, Edinburgh, EH8 9JS, UK

*Corresponding author.

Email addresses: taoyr0601@sjtu.edu.cn (Y. Tao), matthew.brander@ed.ac.uk (M. Brander)

ABSTRACT: The adoption of carbon capture technology in coal-fired power plants is expected to play a pivotal role in the energy transition. This study conducted consequential life cycle assessments (CLCAs) of coal-fired power generation in the United States using policy-level accounting. Monoethanolamine (MEA)-based and Mg-MOF-74-based carbon capture have been introduced, with a comparative analysis conducted on the emissions reduction potential of these two materials through their respective mechanisms of absorption and adsorption. The results indicate that carbon capture based on MEA or Mg-MOF-74 can significantly reduce emissions from coal-fired power generation, decreasing from 779.5 Mt CO_2e to 50.1 Mt CO_2e and 61.1 Mt CO_2e in 2050, respectively. The introduction of ultra-supercritical power plants and carbon capture reduced direct emissions from 92% to 51%. MEA outperforms Mg-MOF-74 slightly, with lower emissions due to solvents and cleaning processes. Deviations in Mg-MOF-74's adsorption capacity and degradation rate could lead to 4%-6% model outcome variations. It is also concluded that the stability of MEA's marginal emissions depends on a steady expansion of existing production capacity, while the marginal emissions of Mg-MOF-74 are anticipated to remain unchanged. This study emphasizes carbon capture's potential but stresses the need for prompt implementation and comprehensive assessments before deployment decisions.

Keywords: Metal-organic frameworks, Monoethanolamine, Life cycle assessment, Carbon capture, Coal-fired power plant, Policy-level accounting

Abbreviations

BAU	Business-As-Usual
CAGR	compound annual growth rate
CLCA	consequential life cycle assessment
DHTA	2,5-dihydroxyterephthalic acid
DMF	dimethylformamide
EtO	ethylene oxide
GHG	greenhouse gas
HSS	heat-stable salts
LCA	life cycle assessment
LCI	life cycle inventory
LCIA	life cycle impact assessment
MEA	monoethanolamine
MOF	metal-organic framework
TSA	temperature swing adsorption

1. Introduction

According to the IPCC, global surface temperatures from 2011 to 2020 were 1.1°C higher compared to the period from 1850 to 1900 (IPCC, 2023). Human-generated greenhouse gas emissions have been identified as the primary driver of global warming, and these emissions continue to rise annually. In recent years, climate-related impacts have been occurring with increasing frequency, such as heatwaves in Europe (Andrews, 2023) and floods in China (Thukral and Qin, 2023), intensifying the call for reducing

greenhouse gas emissions and improving living environments. Among the human-generated greenhouse gas (GHG) emissions, those produced by the energy sector accounted for 31.3% in 2016 (Ritchie et al., 2020). More concerning is that global CO_2 emissions from fossil fuel combustion are still on the rise, experiencing a 1.3% increase of 423 million tonnes in 2022 (IEA, 2023). It has been observed that CO_2 concentrations in atmosphere has increased from 316 ppm in 1960 to 425 ppm in 2024 (Lan and Keeling, 2024). The power sector is a significant contributor to CO_2 emissions, prompting policymakers and researchers to focus on strategies for emissions reduction.

To curb escalating greenhouse gas emissions, it is crucial to boost energy efficiency and transition to cleaner sources. The power generation sector, essential for emissions reduction, must shift predominantly to renewables like solar and wind energy. To expedite this transition and tackle current emissions, immediate measures are essential. Despite carbon capture (CC) having lower potential and higher costs compared to other mitigation actions (IPCC, 2023), its application provides a swift means to reduce global carbon emissions (Li et al., 2022). In 2022, coal constituted 10% of the total energy consumption in the United States, accounting for 27% of the energy consumption within the electric power sector (EIA, 2023c). However, the CO_2 emissions from coal within the electric power sector reached a substantial 53% of total emissions, thereby emphasizing its pronounced carbon intensity (EIA, 2023b). Consequently, carbon capture research predominantly focuses on coal-fired power plants.

The critical role of carbon capture in CO_2 removal has fuelled rapid research, leading to three main methods: pre-combustion, oxy-fuel combustion, and post-combustion. Pre-combustion involves gasifying coal to produce synthesis gas (Chen, 2022), while oxy-fuel combustion reacts coal powder with pure oxygen (Yadav and Mondal, 2022). Post-combustion capture separates CO_2 from flue gas emitted by coal plants, and requires relatively minor modifications to existing coal power plants and is suitable for

retrofitting existing facilities (Chao et al., 2021; Fan et al., 2023). As a result, it has garnered significant attention from researchers in recent years (Fan et al., 2020; Tao and Xu, 2024).

Metal-organic frameworks (MOFs) have been synthesized and extensively studied in recent decades due to their exceptional working adsorption capacities and strong tunability. Currently, numerous MOFs have shown application potential, such as Mg-MOF-74 (Valenzano et al., 2010). Rather than individually experimenting on numerous MOFs to find the ideal material, researchers increasingly employ computational simulations to expedite screening. They typically use adsorption performance indicators, primarily focusing on working capacity and selectivity (Deng et al., 2020; Qiao et al., 2016; Tao et al., 2022). With the proliferation of concepts and methods such as carbon footprint and life cycle assessment (LCA), researchers are also beginning to incorporate the environmental impact into their screening criteria, aiming to identify materials with excellent carbon capture performance and relatively lower environmental costs (Burns et al., 2020; Hu et al., 2021) as well as the performance of retrofitted power plants (Yang et al., 2019). However, due to data availability constraints and future uncertainties, most assessments of MOFs' environmental impact currently focus mainly on their production stage rather than their full life cycle (Grande et al., 2017; Pioquinto-García et al., 2021; Xia et al., 2022). This limited approach can lead policymakers to harbour doubts about the actual emission reduction effects once MOFs are applied in coal-fired power plants.

While prior research has enhanced our understanding of MOFs' environmental impacts, current LCAs on MOFs lack coverage in (1) Emission distribution across their full life cycle, (2) systemic effects of MOFs in coal-fired plants for carbon capture, and (3) comparative emission reduction potential against established materials. This study addresses these gaps by systematically assessing a specific MOF's life cycle emissions,

quantifying the impact of its use in coal-fired plants, and benchmarking against mature carbon capture materials.

2. Methodology

2.1 Goal and Scope Definition

The objective of this study is to conduct consequential life cycle assessments (CLCAs) of emissions reductions achieved by employing two distinct carbon capture materials in all coal-fired power plants in the United States. The carbon accounting methodology employed is a policy-level accounting based on the GHG Protocol's Policy and Action Standard (World Resources Institute, 2014).

The carbon capture materials under discussion includes MEA, which is currently commercially utilized, and Mg-MOF-74, a MOF with significant carbon capture potential. MEA, as an amino material that has been commercially applied, has been used in industry for decades, and its production mode and emissions are relatively stable. Therefore, MEA-based carbon capture is suitable for comparison with MOFs-based carbon capture introduced in recent years to explore the emission reduction potential of current MOFs-based carbon capture technologies. Mg-MOF-74, also termed CPO-27-Mg, is a member of the MOF-74 structural family with Mg as the central metal ion. The structure, like the other materials in the MOF-74 structure series, has a 1-D arrangement of parallel hexagonal channels. Mg-MOF-74 has been widely discussed in recent years because of its high carbon dioxide adsorption capacity and adsorption selectivity at low pressure (Ben-Mansour and Qasem, 2018; DeCoste et al., 2013; Valenzano et al., 2010), and is regarded as an adsorption material with great carbon capture potential. Therefore, this study takes Mg-MOF-74 as a representative of MOFs to explore the emission reduction effect of carbon capture based on Mg-MOF-74.

To comprehensively evaluate the carbon emissions associated with different carbon capture materials from a life cycle perspective, this research scope encompasses various phases throughout the operation of coal-fired power plants. These phases consist of manufacturing (including raw material extraction), transportation, utilization, as well as the recycling and disposal of degraded carbon capture materials.

This study introduces a Business-As-Usual (BAU) scenario and two scenarios with interventions. Each scenario is characterized by distinct descriptions, system boundaries, and emission sources. To facilitate analysis of the respective emission reduction potential and emission sources of MEA and Mg-MOF-74, only one material is used in both scenarios using carbon capture technology. In practice, policymakers can choose a variety of carbon capture materials based on the results, considering different factors such as geographical location, material yield, etc.

BAU scenario: No coal-fired power plants in the United States will be equipped with carbon capture system.

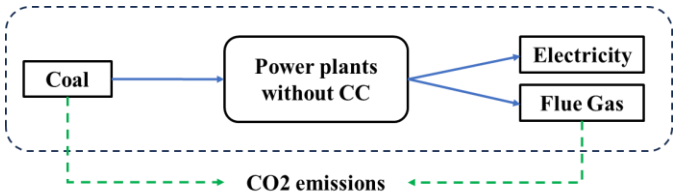

Figure 1 *Schematic diagram of the system boundary and emission sources of the BAU scenario.*

Scenario 1 (MEA-based CC): The carbon capture material for future coal-fired power plants in the United States is MEA.

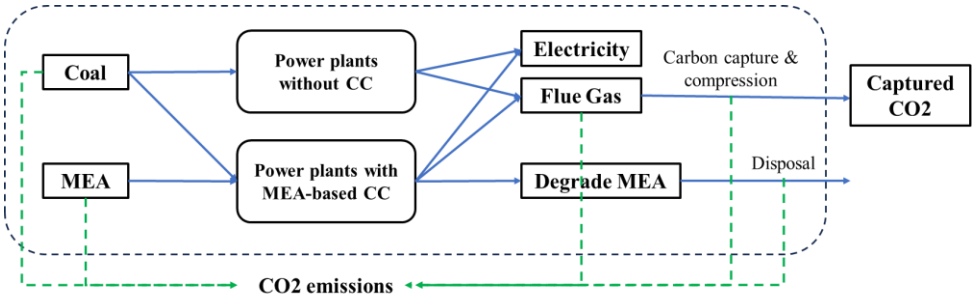

Figure 2 *Schematic diagram of the system boundary and emission sources of Scenario 1.*

Scenario 2 (MOF-based CC): The carbon capture material for future coal-fired power plants in the United States is Mg-MOF-74.

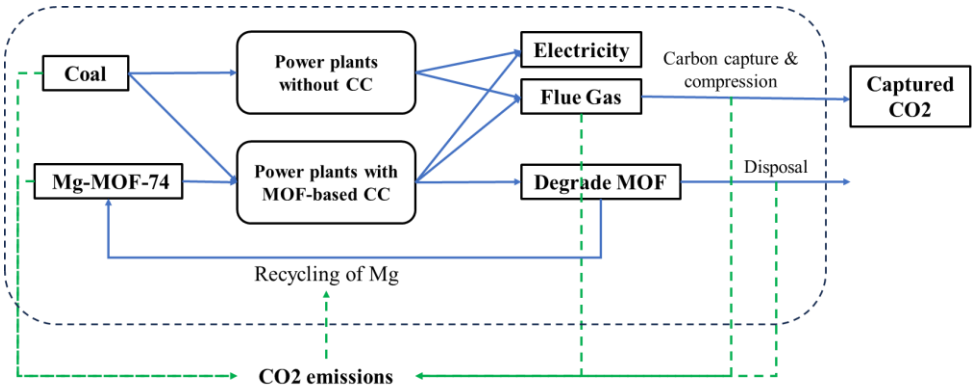

Figure 3 *Schematic diagram of the system boundary and emission sources of Scenario 2.*

It should be noted that the emissions generated during the construction and decommissioning phases of coal-fired power plants are beyond the scope of this study, as the emissions resulting from these activities remain constant across the three scenarios under consideration. Additionally, this study ultimately conducts a comparative analysis of aggregate CO_2 emissions across different years rather than emissions per functional unit at a specific moment. This approach serves to gauge the emission reduction effects of different policy-level interventions.

2.2 Life Cycle Inventory and Data Sources

2.2.1 Coal-Fired Power Plants

Coal-fired power plants are classified into three types: subcritical, supercritical, and ultra-supercritical, based on the differences in the temperature and pressure of their working steam. The technical performance and carbon capture capabilities of coal-fired power plants vary depending on their type. This study is based on the U.S. coal-fired electricity production scenarios proposed by Sathre and Masanet (2013), with adjustments made according to the EIA's coal-fired electricity generation forecasts (EIA, 2023a). Estimates for coal-fired electricity generation in the United States from 2020 to 2050 were derived (as shown in ***Figure 4*** and ***Appendix A***), where the data for the year 2020 was sourced from statistical values provided by Statista (2023). Carbon capture devices are anticipated to be integrated into U.S. coal-fired power plants from 2020 onwards. Subsequently, newly constructed coal-fired power plants will directly deploy carbon capture, while existing plants will gradually retrofit carbon capture devices until all coal-fired power plants have carbon capture by the year 2050.

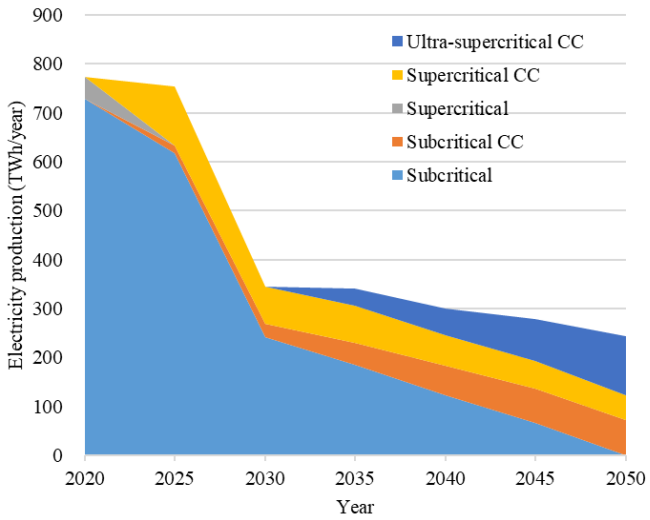

Figure 4 *Illustration of estimated electricity production from coal-fired power plants in the United States from 2020 to 2050.*

For power plants without carbon capture and those with MEA-based carbon capture, the technical parameters (such as coal feed rate and CO_2 emissions) and carbon capture performance estimates are derived from MIT's report for coal-fired power plants with post-combustion carbon capture (Ansolabehere et al., 2007). While for the Mg-MOF-74-based carbon capture power plants, their operational parameters were obtained by adjusting the technical parameters of MEA-based carbon capture power plants from the MIT report, as proposed by Sathre and Masanet (2013). Specific values can be found in ***Appendix B***.

The emissions under the BAU scenario originate from the coal used for electricity generation, which includes emissions from coal mining and transportation, as well as the CO_2 contained in the flue gas generated during the power generation process, as illustrated in ***Figure 1***.

The emissions generated during the coal supply need to be calculated by first determining the annual coal feed amount and then multiplying it by the emission factor of coal:

$$CF_{yr} = \sum CF_i \times E_i \quad (1)$$

$$E_{coal} = CF_{yr} \times EF_{coal} \quad (2)$$

In Equation (1), CF_{yr} represents the annual coal feed amount (in Mt), CF_i denotes the coal demand of power plant i (in t/MWh), and E_i indicates the electricity generation of power plant i in that year. In Equation (2), CE_{coal} represents the emissions from coal supply (in Mt), EF_{coal} represents the emission factor of coal.

All emission factors in this study were sourced from the ReCiPe model in the Ecoinvent v3.9.1 consequential life cycle impact assessment (LCIA) database (Ecoinvent, 2022).

Similar to the calculation method for coal feed, the CO_2 emitted during the power generation process can be obtained based on the CO_2 emissions and electricity production of different coal-fired power plants:

$$E_{emitted} = \sum CE_{e,i} \times E_i \quad (3)$$

In Equation (3), $CE_{e,i}$ indicates the direct emissions of coal-fired power plant i.

2.2.2 MEA-Based Carbon Capture

From a cradle-to-grave life cycle perspective, the emissions associated with post-combustion carbon capture using MEA primarily stem from the supply of MEA, (including its manufacturing and transportation) as well as the energy consumption during MEA utilization for carbon capture and the disposal of degraded MEA.

The presence of free oxygen in flue gas can lead to irreversible oxidative degradation of MEA, resulting in the formation of various degradation products, such as organic acids, ammonia and aldehydes (Bello and Idem, 2005; Gouedard et al., 2012). Consequently, it is necessary to promptly replenish active MEA to the solvent inventory of the capture plant in order to sustain the carbon capture performance. The emissions during the MEA supply phase are determined by the degradation amount of MEA. Based on the pilot data by Moser et al. (2020), the average degradation rate of MEA could achieve 350 g per ton of CO_2 captured. While some scholars have pointed out that this figure may be somewhat optimistic (Weir et al., 2023), it is reasonable to use this already achieved value when predicting its performance over the coming decades in this study. Combining this with the CO_2 capture amount, the annual degradation amount of MEA can be calculated as follows:

$$MEA_{yr} = CE_{captured}/DR_{MEA} \quad (4)$$

$$CE_{captured} = \sum CE_{c,i} \times E_i \quad (5)$$

In Equation (4) and Equation (5), MEA_{yr} refers to the MEA feed in that year, $CE_{captured}$ represents the total amount of CO_2 captured from all coal-fired power plants

in that year, DR_{MEA} refers to the degradation rate of MEA, $CE_{c,i}$ denotes the amount of CO_2 captured by coal-fired power plant i.

As a commercially available product, the emission factor for MEA can be directly obtained from Ecoinvent, which includes emissions associated with its manufacturing and transportation phases. Therefore, the emissions resulting from the supply of MEA are:

$$E_{MEA,supply} = MEA_{yr} \times EF_{MEA} \quad (6)$$

The emissions associated with the use phase of MEA-based carbon capture arise from four activities: coal combustion for power generation, regeneration of MEA, compression of CO_2, and the operation of auxiliary equipment. The required energy for these activities is predominantly derived from the combustion of additional coal, constituting the direct emissions of coal-fired power plants. It is assumed that the regeneration process for the carbon capture material follows the temperature swing regeneration method. In this method, when the MEA absorbs CO_2 to saturation, raising the temperature can release the absorbed CO_2, thereby restoring its carbon capture capacity for reuse. Additionally, after CO_2 is separated from the flue gas, it is often compressed to a certain pressure (typically 150 bar, as discussed by Hu et al. (2021) and Burns et al. (2020)) to facilitate transportation and subsequent storage. It is worth noting that the scope of this study does not encompass the emissions generated from the construction of carbon dioxide transport pipelines, given their relatively minor contribution to total emissions. According to Odeh and Cockerill (2008)'s LCA, emissions from the construction and decommissioning of pipelines, power plants, and capture facilities amount to 3.4 g CO_2e/kWh, approximately 1.3% of the total emissions. Furthermore, the incremental increase in total emissions resulting from adding 100 km of pipeline is only between 0.05% and 0.08%, indicating that the emissions from pipeline construction are not a primary focus for emission reduction.

The consequences of oxidative degradation of MEA necessitate not only the replenishment of active MEA but also the treatment of the degraded solution. The reclamation of MEA can be achieved through methods such as neutralization, ion exchange, thermal reclaiming, among others (Flø et al., 2017). However, due to the lack of specific emission factor data for these MEA regeneration methods, only the disposal of the degraded solution is considered in this study, without incorporating recycling. The emissions resulting from the treatment of the waste solution after MEA degradation are as follows:

$$E_{MEA,disposal} = MEA_{yr} \times EF_{spent\ solvent} \quad (7)$$

Finally, taking into account the coal consumption and direct CO_2 emissions from the coal-fired power plants themselves, the emissions for coal-fired power plants with MEA-based carbon capture is as follows:

$$E_{MEA,total} = E_{coal} + CE_{emitted} + E_{MEA,supply} + E_{MEA,disposal} \quad (8)$$

2.2.3 Mg-MOF-74-Based Carbon Capture

While extensive research has been conducted on Mg-MOF-74 in recent years due to its remarkable carbon dioxide adsorption capacity, the absence of its attainment of commercial application has led to a lack of consensus among researchers and practitioners regarding its life cycle inventory (LCI). In this study, assuming the future potential of Mg-MOF-74 as a post-combustion carbon capture adsorbent, and with the premise of large-scale commercial application utilizing the same synthesis route, a prospective life cycle assessment is carried out for various stages including raw material extraction, manufacturing, transportation, use, recycling, and disposal of Mg-MOF-74.

The first step involves calculating the annual consumption or supply of Mg-MOF-74, which is determined by the degradation ratio and total loading capacity of Mg-MOF-

74 in the power plant. Impurity gases in the flue gas produced after combustion, such as water, SO_2, and NO, can affect the stability of Mg-MOF-74 (Mangano et al., 2016; Tan et al., 2017). Due to the lack of data indicating the degradation rate of Mg-MOF-74 when exposed to flue gas containing both water and SO_2, this study assumes that coal-fired power plants will first remove acidic gases from the flue gas before employing Mg-MOF-74 for carbon capture. This step significantly enhances the durability of Mg-MOF-74. Therefore, if coal-fired power plants adopt Mg-MOF-74 for carbon capture in the future, there is a high probability that the removal of acidic gases will be incorporated into the carbon capture process. The energy consumption associated with this process is include in the energy consumption of carbon capture auxiliary equipment. Based on studies by DeCoste et al. (2013) and Hu et al. (2021), it is assumed that the degradation ratio of Mg-MOF-74 is 3% over a 28-day period. The total loading capacity of Mg-MOF-74 is related to its adsorption rate. The model used in this study adopts the adsorption rate of Mg-MOF-74 in the temperature swing adsorption (TSA) process as obtained by Ben-Mansour and Qasem (2018), which is 0.279 kg CO_2/kg MOF*h. The specific calculation formulas are presented below:

$$MOF_{yr} = Degradation\ ratio \times MOF_{load} \quad (9)$$

$$MOF_{load} = CE_{captured}/AR_{MOF} \quad (10)$$

In Equation (9) and Equation (10), MOF_{yr} represents MOF feed in that year, MOF_{load} represents total loading capacity of MOF in that year, AR_{MOF} represents the adsorption rate of Mg-MOF-74.

The synthesis of all MOFs requires several types of raw materials: metal sources, organic ligand precursors, solvents, and cleaning solutions. Although numerous scholars have investigated the environmental impacts of the manufacturing phase of various MOFs, certain challenges persist. One of the challenges stems from the diversity of synthesis methods and raw materials, leading to the existence of multiple synthesis routes for the same MOF. The environmental impacts of different synthesis

routes reportedly vary significantly (Grande et al., 2017). Furthermore, information regarding energy consumption during material synthesis and solvent cycling is often not provided by the creators of synthesis protocols. Approximately half of MOFs' synthesis protocols only specify the proportions or masses of raw materials without indicating the product's quality, rendering the yield rate unknown (Hu et al., 2021). As a result, in order to estimate the emissions for large-scale production of Mg-MOF-74, certain assumptions need to be made.

In the model constructed for this study, the synthesis protocol of Mg-MOF-74 proposed by Grant Glover et al. (2011) is utilized as a reference. Its LCI is depicted in ***Figure 5***. $Mg(NO_3)_2 \cdot 6H_2O$ is employed as the metal source, 2,5-dihydroxyterephthalic acid (DHTA) serves as the organic ligand precursor, and a mixture of water, dimethylformamide (DMF), and ethanol is utilized as solvents for synthesis. The resulting product is washed using methanol. Grant's protocol specifies the masses of raw materials but does not provide the mass of synthesized Mg-MOF-74. To address this issue, a yield rate of 85% was assumed in this study, and the quantity of Mg-MOF-74 produced was estimated through mass balance and chemical balance calculations. In comparison to laboratory synthesis, industrial-scale production can more efficiently utilize solvents. Therefore, this study referred to the scale-up framework for chemical processes proposed by Piccinno et al. (2016), resulting in a 20% reduction in solvent consumption. Furthermore, considering that methanol, used as cleaning solution, does not directly participate in the synthesis and can be more easily recycled, a 10% reduction in methanol consumption was also assumed.

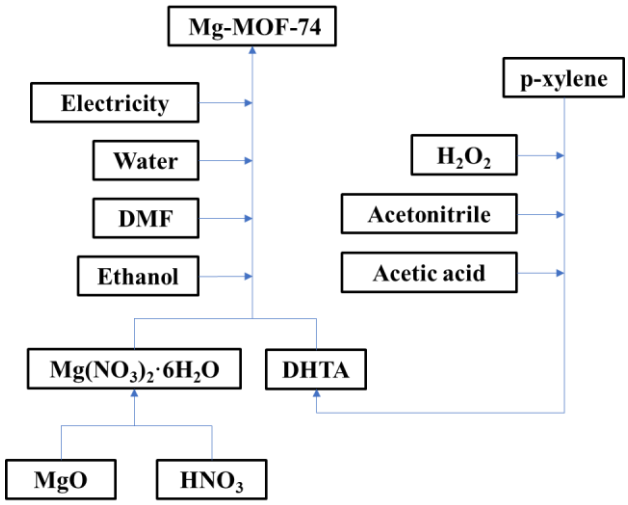

Figure 5 *Schematic diagram of LCI for the synthesis process of Mg-MOF-74.*

However, due to the limited market size of less common chemicals like $Mg(NO_3)_2 \cdot 6H_2O$ and DHTA, there is a lack of LCIA information for them in the Ecoinvent v3.9.1 database. A common approach to address such issues involves approximating their environmental impacts by aggregating the impacts of synthesizing their upstream materials (Galant et al., 2023). For synthesizing $Mg(NO_3)_2 \cdot 6H_2O$, the upstream materials are MgO and HNO_3. The usage of MgO and HNO_3 can be calculated using the following chemical equation balance (assuming no losses in this step):

$$MgO + 2HNO_3 + 5H_2O \rightarrow Mg(NO_3)_2 \cdot 6H_2O$$

According to the DHTA synthesis protocol provided by Li et al. (2016), the required chemicals are p-xylene, hydrogen peroxide (H_2O_2), acetonitrile, and acetic acid. After normalization, the quantity of inputs needed to synthesize 1kg of Mg-MOF-74 is presented in ***Table 1***. It is worth noting that HNO_3 and H_2O_2 are considered in their 100% concentration solutions for the calculations. In addition to the usage of raw materials, the energy consumption required for synthesis also influences the carbon emissions from the production phase. Due to the lack of research on the energy consumption of Mg-MOF-74 synthesis, this study adopts the energy consumption for MOF synthesis as used in the model by Sathre and Masanet (2013), which is 15 GJ per ton of MOF,

equivalent to 4.167 kWh per kilogram of MOF.

Table 1 *Activity data for Mg-MOF-74 in manufacturing phase.*

Function	Inputs	Consumption	Unit
Metal sources: $Mg(NO_3)_2 \cdot 6H_2O$	MgO	0.188	kg/kg Mg-MOF-74
	HNO_3	0.586	
Organic ligand precursor: DHTA	p-xylene	0.860	
	H_2O_2	0.666	
	Acetonitrile	5.493	
	Acetic acid	3.142	
Solvents	DMF	85.430	
	Ethanol	4.760	
	Water	6.033	
Cleaning solutions	Methanol	40.564	
Energy	Electricity	4.167	kWh/kg Mg-MOF-74

To estimate the carbon emissions during the transportation phase of Mg-MOF-74, the first step involves determining its anticipated average transportation distance. In coal-fired power plants in the United States, activated carbon is utilized to adsorb mercury compounds from flue gas (Sjostrom et al., 2010), akin to the function of carbon capture agents. Hence, taking into account the application context of activated carbon, the choice is made to adopt the average transportation distance of activated carbon as a reference for the expected transportation distance of Mg-MOF-74. Based on data from the US Department of Transportation regarding hazardous materials transportation characteristics, statistical information reveals that products falling under the "Class 4, Flammable solids" category, to which activated carbon belongs, are transported an average of 271.81 miles per ton (Duych et al., 2011). Given the absence of specific data concerning the transportation distance of activated carbon, this study elects to utilize the transportation distance associated with the broader "flammable solid" category as a point of reference. Additionally, the assumed mode of transportation is via lorry.

During the usage phase, the LCI of Scenario 2 closely resembles that of Scenario 1.

This encompasses coal combustion for power generation, energy consumption in regenerating the capture material, energy consumption in compressing CO_2, and energy consumption in other auxiliary equipment, all of which are reflected in the direct emissions of coal-fired power plants.

In the LCI of Scenario 2 during the recycling and disposal phase, two key aspects are considered: the recycling of magnesium metal, and the management of discarded chemical compounds. According to a report published by European Commission (2020), the recovered magnesium accounted for 13% of the total magnesium supply. Hence, it is postulated that 13% of the magnesium metal can be extracted from degraded Mg-MOF-74 and reintegrated into the production process of MOFs. The recovered magnesium is assumed to be resold in the market, serving as a form of "substitution" credit to replace/reduce the quantity of "primary" magnesium produced. The remaining unrecovered waste is assumed to be disposed of conventionally, similar to regular disposal of chemical waste.

2.3 Limitations

Model limitations may arise from foundational assumptions. The model exclusively uses MEA or Mg-MOF-74 for carbon capture, applying TSA uniformly for adsorbent regeneration. The novelty of Mg-MOF-74 introduces uncertainty due to its lab-level capacity, and scaling its synthesis aligns with real-world production, acknowledging inherent predictions uncertainty. The chosen synthesis route is one of many, making this a comparative study, not an intrinsic evaluation.

The study also simplifies the separation and refilling process for degraded carbon capture material within beds, overlooking additional processes required based on material attributes. MEA material degradation, resulting from oxidation, leads to

concentration reduction in its liquid state, and heat-stable salts (HSS) generated may cause performance deterioration and equipment issues (Volkov et al., 2014).

The scope focuses solely on emissions (global warming potential), neglecting other environmental impacts (ecotoxicity, acidification, land use). In the studies of MEA's ecotoxicity by Eide-Haugmo et al. (2012) and Libralato et al. (2010), MEA showed slight acute toxicity, and its effective concentration inducing a 50% effect in the observed population (EC-50) value reached 198 mg/l. This emphasizes the necessity for further investigation in this aspect prior to large-scale implementation.

3. Results and Discussion

3.1 Data Presentation

Figure 6 provides a visual representation of the emissions generated by coal-fired power plants operating within the United States under the three scenarios. As time progresses, the total electricity generation experiences a gradual increase to meet the burgeoning demand, as showcased in ***Figure 4***. It is noteworthy that, even in the absence of carbon capture, there is a pronounced decline in total emissions due to the gradual replacement of low-efficiency power plants with high-efficiency counterparts and the diminishing reliance of the power generation industry on coal. The results demonstrate MEA's significant emission cuts in U.S. coal-fired plants, and this advantage continues to escalate with increasing implementation of carbon capture, offering prospects for achieving the net-zero target in the power generation industry.

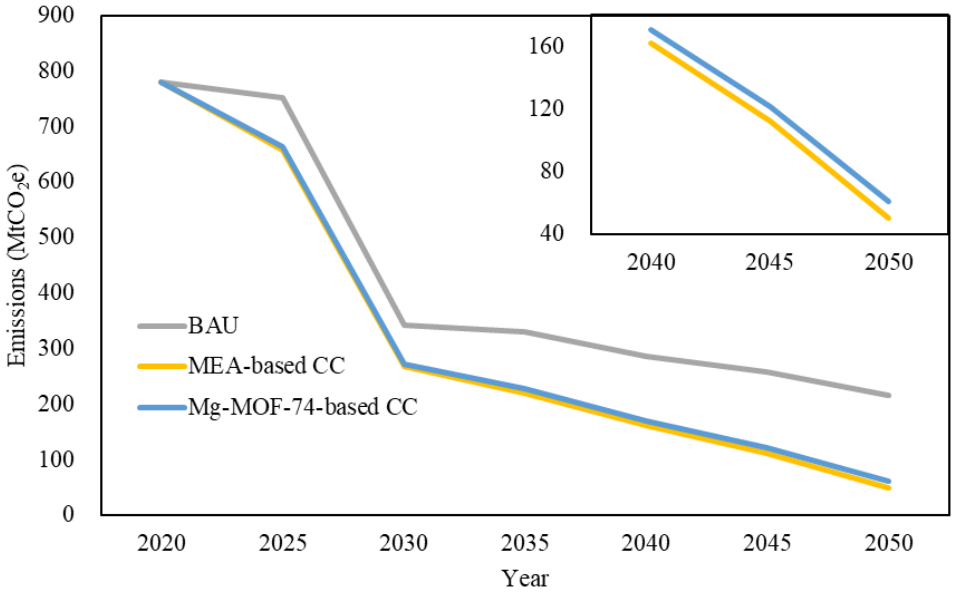

Figure 6 *Illustration of emission reduction performance of MEA-based and Mg-MOF-74-based carbon capture.*

Our analysis starts with the assumption that future U.S. coal-fired power plants won't adopt carbon capture technology, serving as a baseline for evaluating emission reduction methods. ***Table 2*** details relevant data and emissions for this scenario. It is noteworthy that emissions from coal-fired power generation in 2050 are approximately eleven times higher than those from coal supply, emphasizing the dominant role of the operational phase in emissions, aligning with common expectations.

Table 2 *Emission estimates for the BAU scenario.*

	2020	**2025**	**2030**	**2035**	**2040**	**2045**	**2050**
Coal feed (Mt)	315.3	304.5	138.3	133.6	116.3	105.0	87.9
Power plants							
Emissions from coal supply ($MtCO_2e$)	64.9	62.6	28.4	27.5	23.9	21.6	18.1
CO_2 emitted (Mt)	714.7	689.6	312.9	302.1	262.7	237.0	197.9
Total emissions ($MtCO_2e$)	779.5	752.2	341.4	329.6	286.6	258.6	216.0

Table 3 presents emission projections over time in Scenario 1 (deployment of MEA-

based carbon capture). Due to increased coal consumption for powering carbon capture and CO_2 compression, deviating from the BAU scenario, energy demand sees a marginal rise. Despite this, the deployment of MEA-based carbon capture results in a significant 87% reduction in direct CO_2 emissions from power plants by 2050, a stark improvement over the BAU scenario. Although MEA procurement, management, and spent MEA disposal exert some influence, their combined impact remains modest, constituting approximately 1% of total emissions, even with incremental trends until 2050.

Table 3 *Emission estimates for Scenario 1 with MEA-based carbon capture.*

	2020	**2025**	**2030**	**2035**	**2040**	**2045**	**2050**
Coal feed (Mt)	315.3	321.4	151.8	153.0	138.4	130.7	116.3
CO_2 captured (Mt)	0.0	136.1	106.2	155.1	177.1	207.9	233.4
MEA degradation ratio (kg/tCO_2)				0.35			
MEA feed (Mt)	0.00	0.05	0.04	0.05	0.06	0.07	0.08
Power plants & use phase							
Emissions from coal supply (MtCO_2e)	64.9	66.1	31.2	31.5	28.5	26.9	23.9
CO_2 emitted (Mt)	714.7	590.2	236.2	189.0	133.5	84.6	25.7
Raw materials extraction, manufacturing & transportation phase							
Emissions from MEA supply (MtCO_2e)	0.0	0.2	0.1	0.2	0.2	0.2	0.3
Disposal phase							
Emissions from the disposal of degraded MEA (MtCO_2e)	0.0	0.1	0.1	0.1	0.1	0.1	0.2
Total (MtCO_2e)	779.5	656.6	267.6	220.7	162.3	111.8	50.1

The emission outcomes attributed to the utilization of Mg-MOF-74 for carbon capture within coal-fired power plants are succinctly presented in ***Table 4***. Although the employment of Mg-MOF-74 for carbon capture results in slightly less absorption of CO_2 from power plants when contrasted with the MEA-based counterpart, the higher energy consumption in the regeneration of carbon capture materials results in higher

direct emissions from power plants in Scenario 1 as compared to Scenario 2. A comprehensive examination of emissions pertaining to each phase will be expounded upon below.

Table 4 *Emission estimates for Scenario 2 with Mg-MOF-74-based carbon capture.*

	2020	**2025**	**2030**	**2035**	**2040**	**2045**	**2050**
Coal feed (Mt)	315.3	317.2	148.4	147.9	132.5	123.7	108.3
CO_2 captured (Mt)	0.0	127.6	99.4	145.6	166.3	195.5	219.8
Working capacity of Mg-MOF-74 (tCO_2/tMOF)				2444.04			
Loading capacity of MOF (Mt)	0.00	0.05	0.04	0.06	0.07	0.08	0.09
Degradation ratio (%/yr)				39.11%			
MOF feed (Mt)	0.00	0.02	0.02	0.02	0.03	0.03	0.04
Power plants & use phase							
Emissions from coal supply ($MtCO_2e$)	64.9	65.3	30.5	30.4	27.3	25.4	22.3
CO_2 emitted (Mt)	714.7	588.8	235.1	187.8	132.2	83.3	24.5
Raw materials extraction & manufacturing phase							
Emissions from the manufacturing of Mg-MOF-74 (tCO_2e/tMOF)				403.92			
($MtCO_2e$)	0.0	8.2	6.4	9.4	10.8	12.6	14.2
Transportation phase							
Emissions from the transportation of Mg-MOF-74 (tCO_2e/tMOF)				0.06			
($MtCO_2e$)	0.000	0.001	0.001	0.001	0.002	0.002	0.002
Recycling & disposal phase							
Recycling rate of Mg (%)				13%			
Recycled Mg (Mt)	0.0000	0.0002	0.0001	0.0002	0.0002	0.0003	0.0003
Waste (Mt)	0.000	0.020	0.016	0.023	0.026	0.031	0.035
Emissions from the disposal and recycling of Mg-MOF-74 ($MtCO_2e$)	0.000	0.037	0.029	0.042	0.048	0.056	0.063
Total emissions ($MtCO_2e$)	779.5	662.4	272.1	227.7	170.3	121.4	61.1

3.2 Comparison of Emission Contributors

Understanding emissions distribution across diverse carbon capture methods and identifying primary contributors requires a thorough analysis of emission magnitudes. Deconstructing emissions is crucial for gaining valuable insights and paving the way for technological improvements. ***Figure 7*** succinctly illustrates the proportional contributions of various activities to the overall emission composition in Scenario 1.

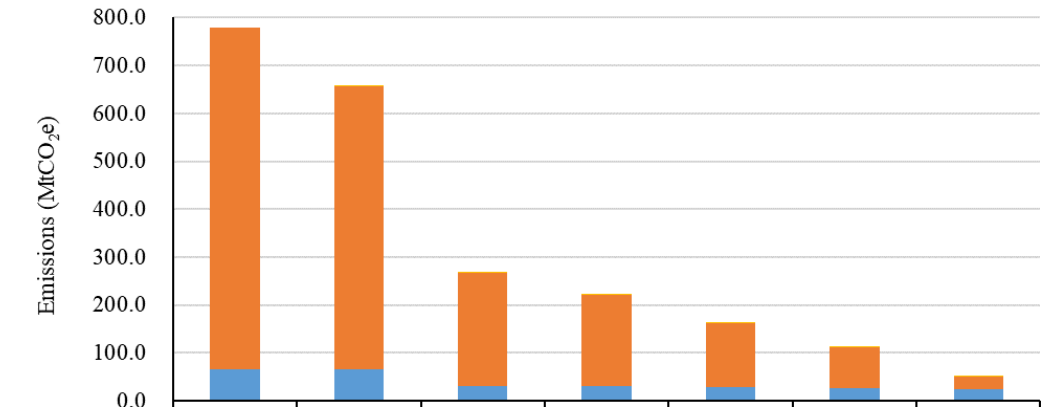

	2020	2025	2030	2035	2040	2045	2050
MEA disposal	0.0	0.1	0.1	0.1	0.1	0.1	0.2
MEA supply	0.0	0.2	0.1	0.2	0.2	0.2	0.3
Power plants	714.7	590.2	236.2	189.0	133.5	84.6	25.7
Coal supply	64.9	66.1	31.2	31.5	28.5	26.9	23.9

Figure 7 *Illustration of Scenario 1 contribution breakdown of emissions (Unit: $MtCO_2e$).*

With the rise of ultra-supercritical power plants and an increase in the implementation of carbon capture, there is projected to be a significant reduction in the previously predominant carbon dioxide emissions. This transition is notably evident, with direct carbon dioxide emissions decreasing from 92% of the total emissions in 2020 to 51% in 2050. This reduction underscores the crucial roles of both advancements in power plants and the adoption of carbon capture technology in mitigating emissions from coal-based power generation, regardless of the specific capture material used.

As carbon capture technology gains momentum in coal-fired power generation, concurrent with increased coal supply and MEA-related emissions, a corresponding rise in emissions is evident. Notably, coal provision's share, which was around 8% in 2020, escalates to approximately 48% by 2050. Addressing this challenge requires strategic improvements in coal extraction and transportation methods for enhanced sustainability. Conversely, emissions from MEA supply and waste management remain comparatively modest, suggesting potential for further exploration of ancillary environmental impacts associated with MEA utilization. Future investigations can delve into these aspects while acknowledging the evolving landscape of carbon capture in coal-fired power plants.

Figure 8 presents the magnitude of different emission sources within Scenario 2 (deployment of MOF-based carbon capture). When contrasted with Scenario 1, the emissions originating from power generation and coal supply in Scenario 2 exhibit relatively diminished numerical values, although the disparity between the two remains small. Nonetheless, akin to Scenario 1, emissions from power generation and coal supply sustain their primacy as principal contributors to total emissions. Despite witnessing gradual abatement, these two activities are anticipated to collectively contribute to more than 75% of total emissions by the year 2050.

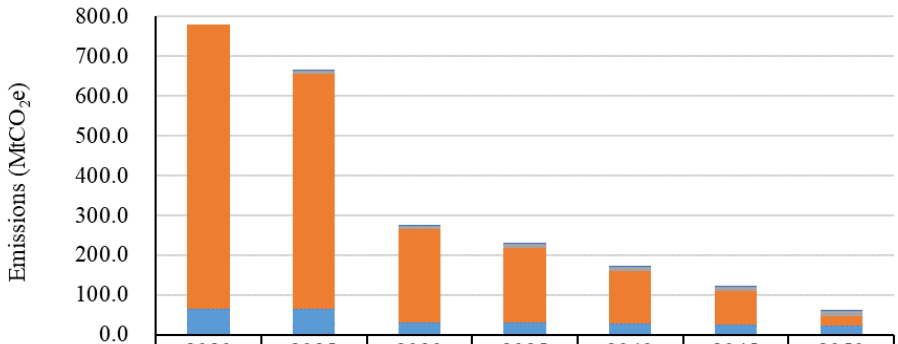

	2020	2025	2030	2035	2040	2045	2050
MOF recycling & disposal	0.000	0.037	0.029	0.042	0.048	0.056	0.063
MOF transportation	0.000	0.001	0.001	0.001	0.002	0.002	0.002
MOF manufacturing	0.0	8.2	6.4	9.4	10.8	12.6	14.2
Power plants	714.7	588.8	235.1	187.8	132.2	83.3	24.5
Coal supply	64.9	65.3	30.5	30.4	27.3	25.4	22.3

Figure 8 *Illustration of Scenario 2 contribution breakdown of emissions (Unit: MtCO2e).*

Moreover, as carbon capture technology garners wider adoption within the coal-fired power generation sector, the requisition for Mg-MOF-74 experiences a marked escalation in Scenario 2. It is worth noting that the manufacture of Mg-MOF-74, including the extraction of raw materials, is associated with relatively elevated emissions, estimated at approximately 403.92 kg CO_2/kg. This stands in stark contrast to the emissions stemming from MEA supply, measured at 3.184 kg CO_2/kg by Ecoinvent (2022). Consequently, the emissions attributed to the production of Mg-MOF-74 substantively contribute, encompassing more than 20% of the cumulative emissions in 2050 when carbon capture technologies are widely implemented. In comparison, emissions originating from the phases of transportation, recycling, and disposal of Mg-MOF-74 exhibit negligible proportions when juxtaposed against other operational activities. This delineates a clear trajectory for future investigation, underscoring the imperative of refining production protocols for novel carbon capture materials like Mg-MOF-74. A targeted approach could encompass the judicious selection of more ecologically suitable raw materials, thereby facilitating a reduction in the lifecycle emissions associated with the resultant product.

To identify key emission contributors in the current synthesis of Mg-MOF-74, a crucial dissection analysis of manufacturing emissions, illustrated in ***Figure 9***, is essential. Solvents stand out as the primary emission source, followed by cleaning solutions and organic ligand precursors. This deduction aligns with other scholars' research (Grande et al., 2017; Pioquinto-García et al., 2021), reinforcing credibility.

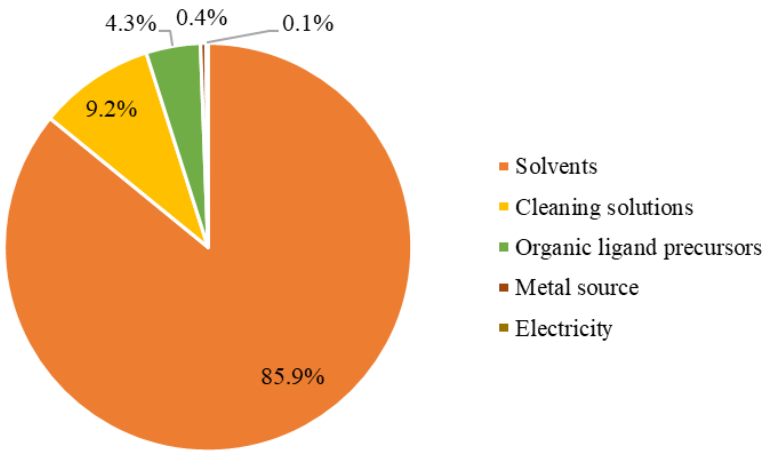

Figure 9 *Emission composition during the manufacturing phase of Mg-MOF-74.*

This finding assumes paramount significance, as it offers material scientists valuable insights for prioritizing the adoption of chemicals characterized by diminished environmental impacts during the formulation of novel synthesis protocols. It is worthwhile to note that emissions stemming from metal sources and energy consumption exhibit a relatively small footprint, and are not the priority areas for abatement action.

3.3 Sensitivity Analysis

Conducting a vital sensitivity analysis enhances the model's comprehension of key parameters and reveals significant variables impacting outcomes. Given MEA's mature commercial status, fewer assumptions were required for the calculations for Scenario

1. Therefore, the sensitivity analysis focuses on Scenario 2, employing Mg-MOF-74 for carbon capture, particularly examining the emissions landscape in 2050. The analysis scrutinizes critical parameters—degradation ratio, transportation distance, and solvent consumption reductions. Each parameter is adjusted positively and negatively by 20%, and resulting 2050 emissions are systematically documented. ***Table 5*** and ***Figure 10*** present insights derived from this analysis.

Table 5 *Sensitivity analysis of key parameters in the model. Base case CO_2e in 2050: 61.09 Mt.*

	Base value	**+20% value**	**+20% CO_2e**	**% change**	**-20% value**	**-20% CO_2e**	**% change**
Degradation ratio in 28 days	3%	3.6%	63.94	4.67%	2.4%	58.23	-4.67%
Distance transported (miles/tMOF)	271.81	326.17	61.09	~0%	217.44	61.09	~0%
Reduction in solvent consumption (%)	20%	24%	60.41	-1.11%	16%	61.76	1.11%
Recycling loss of cleaning solutions (%)	10%	12%	61.35	0.43%	8%	60.82	-0.43%
Yield loss (%)	15%	18%	61.60	0.85%	12%	60.60	-0.79%
Working capacity ($kgCO_2$/kg MOF*h)	0.279	0.335	58.71	-3.89%	0.223	64.65	5.84%
Electricity consumption in synthesis (kWh/kg MOF)	4.167	5.000	61.09	0.01%	3.334	61.08	-0.01%
Recycling loss of metal (%)	13%	15.6%	61.08	~0%	10.4%	61.09	~0%

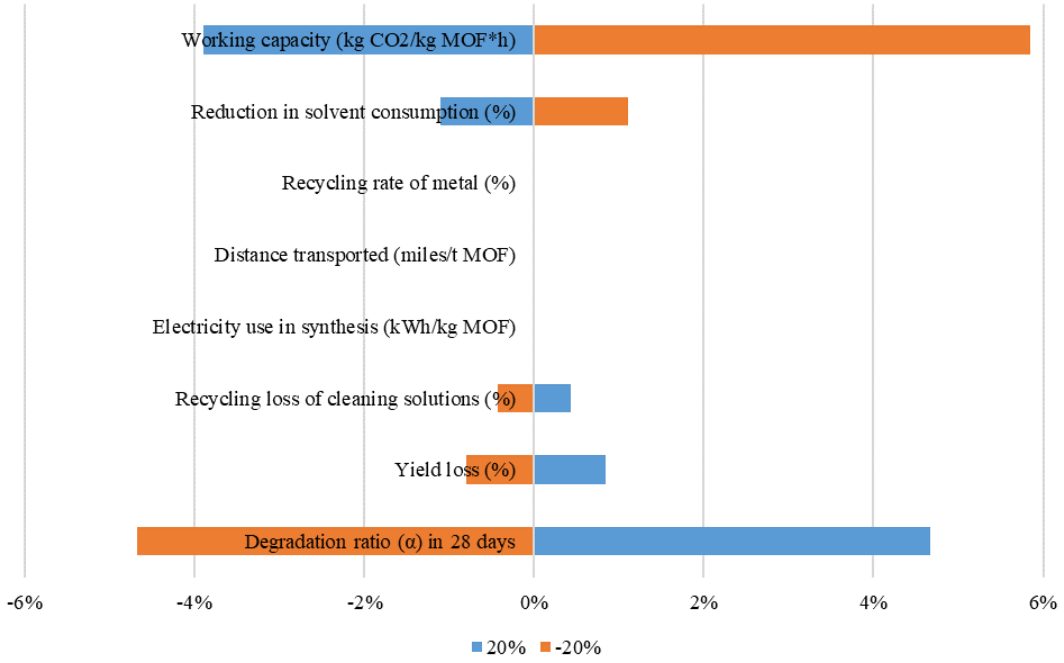

Figure 10 *Tornado diagram: results of sensitivity analysis.*

Deviations in Mg-MOF-74's adsorption capacity significantly impact model outcomes. A negative 20% capacity deviation could increase 2050 emissions by 5.84%, equivalent to 3.57 million tonnes of CO_2. Conversely, underestimating adsorption by a factor 20% may lead to a 3.89% reduction in model results. This emphasizes the critical role of selecting the right carbon capture material for emissions reduction in coal-fired power plants. Achieving targeted adsorption hinges on product quality, carbon capture bed design, and regular maintenance. As industrial production and deployment of materials like Mg-MOF-74 progress, rigorous quality assessment and routine maintenance become imperative for optimal capture media utilization.

Fluctuations in the degradation ratio of Mg-MOF-74 also has substantial influence over the model's projections. A 20% change in this parameter leads to a substantial 4.67% deviation in total emissions, resulting in an additional discharge of around 2.85 Mt CO_2e. Consequently, during the process of MOF selection for carbon capture purposes, it becomes paramount to account for the stability of the material under consideration.

Furthermore, the prudent inclusion of supplementary materials or processes, specifically aimed at fortifying material stability and augmenting durability, should be integrated into the strategic blueprint of carbon capture technologies. This holistic approach serves to enhance the reliability and sustainability of the chosen materials, ensuring their consistent performance and extended serviceability over time.

Remarkably, fluctuations in synthesis energy consumption do not seem to exert a substantial influence on the model's outcomes. It is worth noting that investigations into various synthesis protocols for MOFs frequently omit the provision of energy consumption data within their reports. This data gap leaves researchers grappling with vague suppositions or necessitates intricate computations, thereby fostering an expanse of uncertainty spanning from 0.27 GJ/t to 61 GJ/t (Sathre and Masanet, 2013). Nonetheless, the sensitivity analysis conducted as part of this study implies that the eventual emission outcomes exhibit a degree of resistance in the face of the uncertainty associated with the synthesis energy consumption of MOFs. This observation highlights the relatively moderate impact of energy consumption variations on the overall emissions projection calculated by the model.

The recovery of magnesium from degraded Mg-MOF-74 was modelled using the substitution method, i.e. credit is given for the avoided emissions from primary magnesium production that is avoided due to the supply of recovered magnesium. Consequently, the achieved negative emission from magnesium recovery amounted to 0.006 million tonnes in 2050. In the same year, Mg-MOF-74 is estimated to consume 0.04 million tonnes, less than MEA's 0.08 million tonnes. Prioritizing MOFs with high-emission metal atoms for carbon capture node selection to boost recycling phase performance is discouraged. Such an approach is foreseen to escalate emissions in the MOF's manufacturing, ultimately raising overall emissions.

Based on the results of sensitivity analysis, adjustments were made to the parameters with the most significant impact on the model results, namely the degradation ratio and working capacity. The upper and lower bounds of Scenario 2 were obtained, as shown in ***Figure 11***. Interestingly, even when the degradation ratio of Mg-MOF-74 was reduced by 20%, the total emissions from coal-fired power plants remained higher than in Scenario 1 with MEA-based carbon capture. This outcome highlights the current advantage of MEA and serves as a reminder for the development of MOFs for carbon capture. MOFs like Mg-MOF-74, which are widely recommended, may not necessarily exhibit as much emission reduction potential as their working capacity suggests. Therefore, when selecting adsorbent materials, conducting forward-looking LCAs to assess their true emission reduction capabilities is essential.

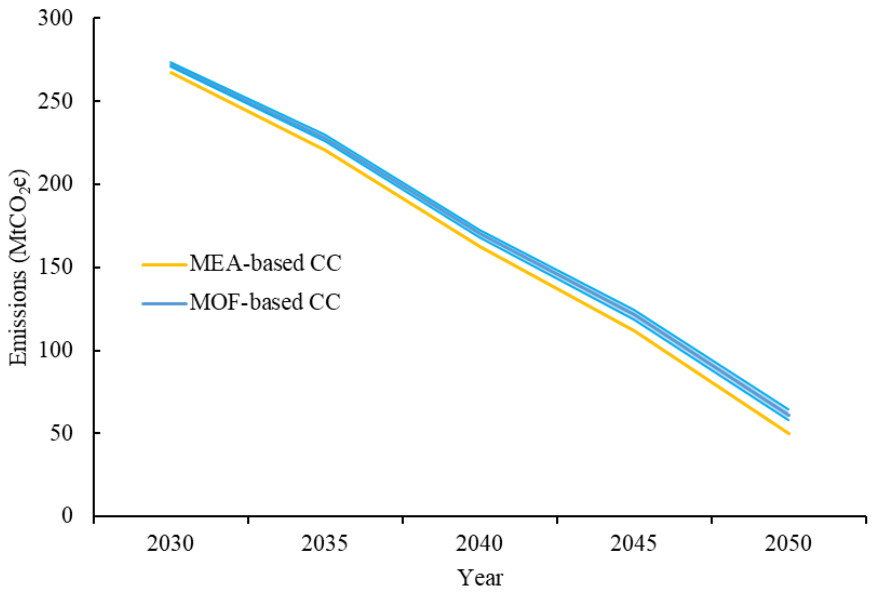

Figure 11 *Illustration of the upper and lower bounds of Scenario 2.*

3.4 Marginal Systems

To ensure the stability of the model results, this study attempted to identify whether the marginal suppliers of several raw materials would undergo changes in the future as

demand increases. The goal was to determine whether such changes could significantly bias the model results. It should be emphasized, however, that the discussion of marginal systems here is based on the way in which the future production of MEA and Mg-MOF-74 are based on the assumptions of this study.

3.4.1 Marginal System of MEA

The supply chain for MEA originates from crude oil and natural gas, with the United States being a global leader in both of these products. In 2022, the United States was the world's largest crude oil producer with a production of 762 million tonnes, followed by Saudi Arabia and Russia, which produced 601 million tonnes and 539 million tonnes, respectively (Enerdata, 2023). In 2022, the United States also held the highest natural gas production in the world, reaching 1027 billion cubic meters (Enerdata, 2023). This production level significantly surpassed the second-ranked country, Russia, which produced 699 billion cubic meters (Enerdata, 2023). Although there is currently no shortage of oil and gas used to produce MEA, it is important to note that as net-zero emissions targets approach, increasing pressure to reduce emissions will be passed on to the production of MEA with oil and gas as raw materials. At that time, it may be necessary to use lower emission production methods to meet emission requirements. This may lead to marginal emissions changes in MEA supply in Scenario 1 or even a risk of MEA supply shortage.

After the extraction of oil and natural gas, the next step involves using steam cracking to produce ethylene from these hydrocarbons, and steam reforming to produce hydrogen gas. According to the Essential Chemistry Industry website, approximately 60% of the produced ethylene is eventually converted into polyethylene, while around 16% is transformed into ethylene oxide (EtO), which is a crucial chemical in the production of MEA (ECI, 2017). In 2018, the United States produced 2.8 million tonnes of ethylene oxide, accounting for 10.9% of the global EtO production (Statista, 2020).

Ammonia is another vital component in the production of MEA, and its chemical synthesis heavily depends on hydrogen and nitrogen. According to the EIA, the United States ranked third in global ammonia production in 2021, following China and Russia (EIA, 2021). Additionally, the carbon intensity of ammonia production has exhibited a decreasing trend in recent years (EIA, 2021). Lastly, the reaction of ammonia with ethylene oxide yields MEA, diethanolamine, and triethanolamine. The proportions of these products can be regulated by adjusting the ratios of the reactants. In 2023, the global production of MEA reached 2.04 million tonnes (EMR, 2023).

In the model for this study, the application of MEA-based carbon capture in coal-fired power plants results in an increasing annual demand for MEA. Currently, the United States accounts for less than 5% of the global MEA consumption (EMR, 2023; U.S. Department of Energy, 2022). According to the projections of this study, the demand for MEA utilized in carbon capture for coal-fired power plants is expected to increase to 0.08 million tonnes by 2050 at a compound annual growth rate (CAGR) not exceeding 8%. Given the current technological maturity of MEA and the abundance of upstream raw materials (petroleum and natural gas) in the United States, meeting this increased demand appears relatively feasible. Therefore, if MEA continues to be employed as a carbon capture material for coal-fired power plants in the coming decades, it necessitates a gradual expansion of existing production capacities to meet demand, thereby avoiding significant fluctuations in prices and marginal emissions. It is worth noting that as MEA's production chain involves numerous chemicals with diverse applications, a more comprehensive analysis is essential to fully comprehend the cascading effects of increased MEA demand.

Table 6 *Trend of MEA consumption for Scenario 1 from 2020 to 2050.*

	2020	**2025**	**2030**	**2035**	**2040**	**2045**	**2050**

MEA feed (Mt)	0.00	0.05	0.04	0.05	0.06	0.07	0.08
CAGR (%)	/	/	-4.8%	7.9%	2.7%	3.3%	2.3%

3.4.2 Marginal System of MgO

MgO serves as the precursor for the metal atoms in the synthesis of Mg-MOF-74, and any shifts in the marginal suppliers of MgO undeniably hold the potential to impact the emission outcomes of Mg-MOF-74. In 2022, the magnesium compound production in the United States amounted to the equivalent of 450,000 metric tons of MgO, with 67% of this production sourced from seawater and natural brines (U.S. Geological Survey, 2023). However, due to the relatively high demand for magnesium compounds in the U.S., domestic production falls short of meeting the requirements, leading to the necessity of importing magnesium compounds from other countries. According to statistics from the U.S. Geological Survey, in 2022, the United States imported a total of 640,000 metric tons of magnesium compounds from other countries (U.S. Geological Survey, 2023). These suppliers can be regarded as the current marginal suppliers of magnesium compounds for the United States. Notably, China stands as the largest exporter of magnesium compounds to the United States, accounting for 61% of the total import volume from 2018 to 2021, with Israel being the second-largest exporter at 10% (U.S. Geological Survey, 2023).

If Mg-MOF-74 is used as the carbon capture material for U.S. coal-fired power plants, the estimated consumption of MgO for producing Mg-MOF-74 in 2050 would reach 6,600 metric tons, approximately 1% of the import volume in 2022. If 13% of the metal in the degraded MOF is recycled, this figure can be reduced to approximately 6,000 metric tonnes. Therefore, under Scenario 2, with the increasing demand for MgO, the U.S. import volume of magnesium compounds would also gradually rise, but the growth rate would be much lower than the increase in MEA demand in Scenario 1. Additionally, as the largest exporter of magnesium compounds to the U.S., China's magnesium production showed an upward trend with an export of 497,700 metric tons

of magnesium products in 2022 (SunSirs, 2023). Based on this information, it can be tentatively concluded that the rising demand for MgO in the U.S. can be met by its main supplier, China, without considering unforeseen policy interventions. The stability of the marginal supplier implies that emissions will not undergo significant changes due to a shortage in the supply of this material.

4. Conclusions

In this study, a forward-looking cradle-to-grave consequential LCA to evaluate carbon capture based on both MEA and Mg-MOF-74 was employed, encompassing activities ranging from coal supply to power plants, direct CO_2 emissions, and the extraction, production, transportation, recycling, and waste management of carbon capture materials.

Compared to Mg-MOF-74-based carbon capture, MEA-based carbon capture shows the potential to help further reduce emissions from coal-fired power generation in the United States at a time when coal generation is declining year by year. It can also be expected that the mature and stable MEA supply chain will add convenience to the implementation of MEA-based carbon capture technology. It is anticipated that the emissions attributed to coal-fired power generation in the United States in 2050 could reach 50.1 million tons, significantly lower than the 216 million tons projected under the BAU scenario. The reduction in emissions resulting from MEA-based carbon capture primarily stems from a substantial decrease in direct CO_2 emissions from coal-fired power plants, far surpassing the additional emissions associated with the production, transportation, and disposal of MEA. While this scenario could help achieve emissions reduction targets more quickly, there are some considerations that need to be considered. Given the potential of MEA as a major emission reduction material, current global and domestic production of MEA may need to be further

ramped up to meet future demand. Although the potential for capacity expansion appears feasible, given a maximum 8% CAGR and abundant upstream resources, there are associated risks of price fluctuations and variability in marginal emissions. If more advanced amine-based capture technology with stronger carbon capture capacity, lower energy consumption and lower consumption rate is adopted, the emission reduction potential can be further improved. In addition, oil and gas as raw materials of MEA may face supply constraints in the future, so the production method of MEA may change, which will bring challenges to the supply of MEA. MEA's ecotoxicity is also an issue that needs to be addressed properly.

The emissions resulting from the utilization of Mg-MOF-74 for carbon capture primarily arise from the production process of the MOF. In Scenario 2, the emissions associated with the production of Mg-MOF-74 for carbon capture in U.S. coal-fired power plants are projected to reach 14.2 million tons of CO_2e in 2050. Chemicals used in production, especially solvents and cleaning solutions, contribute to this. Adopting cleaner synthesis or alternative chemicals can significantly reduce Mg-MOF-74 emissions. Despite reliance on imports from China, the current supply in the U.S. for MgO (the precursor of Mg-MOF-74) can meet Scenario 2's demand. This stability of supply aids LCA research and policymaking, ensuring accurate assessments for informed decisions on power plant retrofitting and carbon capture material planning. The working adsorption capacity and degradation ratio of Mg-MOF-74 directly impact carbon capture in power plants. Deviations may require increased Mg-MOF-74 supply. Furthermore, deviations between assumed parameter values and actual conditions can impact emissions. A 20% decrease in the working capacity of Mg-MOF-74 results in a 3.57 Mt CO_2e increase in total coal-fired power generation emissions by 2050, while a 20% increase in degradation rate leads to a 2.85 Mt CO_2e rise in total emissions by the same year. It should also be noted that the parameters used in estimating the emission performance of MOFs-based carbon capture in this study are mostly based on existing

researches. However, as MOFs-based carbon capture is an emerging technology, there is still potential for further improvement in process parameters. Therefore, its emission reduction capacity compared to MEA-based carbon capture is expected to be further enhanced.

Acknowledgements

This research did not receive any specific grant from funding agencies in the public, commercial, or not-for-profit sectors.

References

Andrews, M., 2023. Weather tracker: temperatures to intensify in Europe as new heatwave hits, Guardian.

Ansolabehere, S., Beer, J., Deutch, J., Ellerman, A.D., Friedmann, S.J., Herzog, H., Jacoby, H.D., Joskow, P.L., McRae, G., Lester, R., Moniz, E.J., Steinfeld, E., 2007. The Future of Coal. Massachusetts Institute of Technology.

Bello, A., Idem, R.O., 2005. Pathways for the Formation of Products of the Oxidative Degradation of CO_2-Loaded Concentrated Aqueous Monoethanolamine Solutions during CO_2 Absorption from Flue Gases. Industrial & Engineering Chemistry Research 44(4), 945-969.

Ben-Mansour, R., Qasem, N.A.A., 2018. An efficient temperature swing adsorption (TSA) process for separating CO_2 from CO_2/N_2 mixture using Mg-MOF-74. Energy Conversion and Management 156, 10-24.

Burns, T.D., Pai, K.N., Subraveti, S.G., Collins, S.P., Krykunov, M., Rajendran, A., Woo, T.K., 2020. Prediction of MOF Performance in Vacuum Swing Adsorption Systems for Postcombustion CO_2 Capture Based on Integrated Molecular Simulations, Process Optimizations, and Machine Learning Models. Environmental Science & Technology 54(7), 4536-4544.

Chao, C., Deng, Y., Dewil, R., Baeyens, J., Fan, X., 2021. Post-combustion carbon capture. Renewable and Sustainable Energy Reviews 138, 110490.

Chen, Z., 2022. A Review of Pre-combustion Carbon Capture Technology, Proceedings of the 2022 7th International Conference on Social Sciences and Economic Development (ICSSED 2022). Atlantis Press, pp. 524-528.

DeCoste, J.B., Peterson, G.W., Schindler, B.J., Killops, K.L., Browe, M.A., Mahle, J.J., 2013. The effect of water adsorption on the structure of the carboxylate containing metal–organic frameworks Cu-BTC, Mg-MOF-74, and UiO-66. Journal of Materials Chemistry A 1(38), 11922-11932.

Deng, X., Yang, W., Li, S., Liang, H., Shi, Z., Qiao, Z., 2020. Large-Scale Screening and Machine Learning to Predict the Computation-Ready, Experimental Metal-Organic Frameworks for CO_2 Capture from Air. Applied Sciences 10(2), 569.

Duych, R., Ford, C., Sanjani, H., 2011. Hazardous Materials Highlights: 2007 Commodity Flow Survey.

ECI, 2017. Ethene (Ethylene). https://www.essentialchemicalindustry.org/chemicals/ethene.html. (Accessed 13/08 2023).

Ecoinvent, 2022. Lifecycle Inventories Database v3.9.1. Switzerland.

EIA, 2021. Natural Gas Weekly Update. https://www.eia.gov/naturalgas/weekly/archivenew_ngwu/2021/04_01/#:~:text=Ammonia%20is%20produced%20at%2032,million%20mt%2Fy%20in%202020.

EIA, 2023a. ANNUAL ENERGY OUTLOOK 2023.

EIA, 2023b. How much of U.S. carbon dioxide emissions are associated with electricity

generation? https://www.eia.gov/tools/faqs/faq.php?id=77&t=11. 2023).
EIA, 2023c. U.S. energy consumption by source and sector, 2022.
Eide-Haugmo, I., Brakstad, O.G., Hoff, K.A., da Silva, E.F., Svendsen, H.F., 2012. Marine biodegradability and ecotoxicity of solvents for CO_2-capture of natural gas. International Journal of Greenhouse Gas Control 9, 184-192.
EMR, 2023. Global Monoethanolamine Market Outlook. Expert Market Research.
Enerdata, 2023. World Energy & Climate Statistics – Yearbook 2023.
European Commission, 2020. Study on the EU's list of Critical Raw Materials - Final Report (2020).
Fan, J.-L., Fu, J., Zhang, X., Li, K., Zhou, W., Hubacek, K., Urpelainen, J., Shen, S., Chang, S., Guo, S., Lu, X., 2023. Co-firing plants with retrofitted carbon capture and storage for power-sector emissions mitigation. Nature Climate Change 13(8), 807-815.
Fan, J.-L., Xu, M., Wei, S., Shen, S., Diao, Y., Zhang, X., 2020. Carbon reduction potential of China's coal-fired power plants based on a CCUS source-sink matching model. Resources Conservation and Recycling, 105320.
Flø, N.E., Faramarzi, L., de Cazenove, T., Hvidsten, O.A., Morken, A.K., Hamborg, E.S., Vernstad, K., Watson, G., Pedersen, S., Cents, T., Fostås, B.F., Shah, M.I., Lombardo, G., Gjernes, E., 2017. Results from MEA Degradation and Reclaiming Processes at the CO_2 Technology Centre Mongstad. Energy Procedia 114, 1307-1324.
Galant, O., Aborome, A., McCalmont, A.S., James, S.L., Patrascu, M., Spatari, S., 2023. LCA as a Tool to Detect Environmental “Hot Spots” in Early-Stage Mechanochemical Synthesis of Organic Dyes. ACS Sustainable Chemistry & Engineering.
Gouedard, C., Picq, D., Launay, F., Carrette, P.L., 2012. Amine degradation in CO_2 capture. I. A review. International Journal of Greenhouse Gas Control 10, 244-270.
Grande, C.A., Blom, R., Spjelkavik, A., Moreau, V., Payet, J., 2017. Life-cycle assessment as a tool for eco-design of metal-organic frameworks (MOFs). Sustainable Materials and Technologies 14, 11-18.
Grant Glover, T., Peterson, G.W., Schindler, B.J., Britt, D., Yaghi, O., 2011. MOF-74 building unit has a direct impact on toxic gas adsorption. Chemical Engineering Science 66(2), 163-170.
Hu, J., Gu, X., Lin, L.-C., Bakshi, B.R., 2021. Toward Sustainable Metal–Organic Frameworks for Post-Combustion Carbon Capture by Life Cycle Assessment and Molecular Simulation. ACS Sustainable Chemistry & Engineering 9(36), 12132-12141.
IEA, 2023. CO_2 Emissions in 2022. IEA, Paris.
IPCC, 2023. Climate Change 2023: Synthesis Report. IPCC.
Lan, X., Keeling, R., 2024. Trends in Atmospheric Carbon Dioxide (CO_2). https://gml.noaa.gov/ccgg/trends/data.html.
Li, K., Shen, S., Fan, J.-L., Xu, M., Zhang, X., 2022. The role of carbon capture, utilization and storage in realizing China's carbon neutrality: A source-sink matching analysis for existing coal-fired power plants. Resources, Conservation and Recycling 178, 106070.
Li, Y., Duan, D., Wu, M., Li, J., Yan, Z., Wang, W., Zi, G., Wang, J., 2016. One-step

synthesis of 2,5-dihydroxyterephthalic acid by the oxidation of p-xylene over M-MCM-41 (M=Fe, Fe/Cu, Cu) catalysts. Chemical Engineering Journal 306, 777-783.
Libralato, G., Volpi Ghirardini, A., Avezzù, F., 2010. Seawater ecotoxicity of monoethanolamine, diethanolamine and triethanolamine. Journal of Hazardous Materials 176(1), 535-539.
Mangano, E., Kahr, J., Wright, P.A., Brandani, S., 2016. Accelerated degradation of MOFs under flue gas conditions. Faraday Discussions 192(0), 181-195.
Moser, P., Wiechers, G., Schmidt, S., Garcia Moretz-Sohn Monteiro, J., Charalambous, C., Garcia, S., Sanchez Fernandez, E., 2020. Results of the 18-month test with MEA at the post-combustion capture pilot plant at Niederaussem – new impetus to solvent management, emissions and dynamic behaviour. International Journal of Greenhouse Gas Control 95, 102945.
Odeh, N.A., Cockerill, T.T., 2008. Life cycle GHG assessment of fossil fuel power plants with carbon capture and storage. Energy Policy 36(1), 367-380.
Piccinno, F., Hischier, R., Seeger, S., Som, C., 2016. From laboratory to industrial scale: a scale-up framework for chemical processes in life cycle assessment studies. Journal of Cleaner Production 135, 1085-1097.
Pioquinto-García, S., Rosas, J.M., Loredo-Cancino, M., Giraudet, S., Soto-Regalado, E., Rivas-García, P., Dávila-Guzmán, N.E., 2021. Environmental assessment of metal-organic framework DUT-4 synthesis and its application for siloxane removal. Journal of Environmental Chemical Engineering 9(6), 106601.
Qiao, Z., Zhang, K., Jiang, J., 2016. In silico screening of 4764 computation-ready, experimental metal–organic frameworks for CO_2 separation. Journal of Materials Chemistry A 4(6), 2105-2114.
Ritchie, H., Rosado, P., Roser, M., 2020. Emissions by sector: where do greenhouse gases come from? Our World in Data.
Sathre, R., Masanet, E., 2013. Prospective life-cycle modeling of a carbon capture and storage system using metal–organic frameworks for CO 2 capture. RSC advances 3(15), 4964-4975.
Sjostrom, S., Durham, M., Bustard, C.J., Martin, C., 2010. Activated carbon injection for mercury control: Overview. Fuel 89(6), 1320-1322.
Statista, 2020. Ethylene oxide production in the United States from 1990 to 2019. Statista.
Statista, 2023. Net electricity generation in the United States from 1990 to 2022, by energy source.
SunSirs, 2023. SunSirs: From January to December 2022, China Exported 497700 Tons of Various Magnesium Metal Products. https://www.sunsirs.com/uk/detail_news-10780.html. (Accessed 13/08 2023).
Tan, K., Zuluaga, S., Wang, H., Canepa, P., Soliman, K., Cure, J., Li, J., Thonhauser, T., Chabal, Y.J., 2017. Interaction of Acid Gases SO2 and NO2 with Coordinatively Unsaturated Metal Organic Frameworks: M-MOF-74 (M = Zn, Mg, Ni, Co). Chemistry of Materials 29(10), 4227-4235.

Tao, Y.R., Xu, H.J., 2024. A critical review on potential applications of Metal-Organic frameworks (MOFs) in adsorptive carbon capture technologies. Applied Thermal Engineering 236, 121504.
Tao, Y.R., Zhang, G.H., Xu, H.J., 2022. Grand canonical Monte Carlo (GCMC) study on adsorption performance of metal organic frameworks (MOFs) for carbon capture. Sustainable Materials and Technologies 32, e00383.
Thukral, N., Qin, N., 2023. China floods hit rice, corn crops; trigger food inflation worries, Reuters.
U.S. Department of Energy, 2022. Carbon Capture, Transport, & Storage Supply Chain Deep Dive Assessment.
U.S. Geological Survey, 2023. Mineral commodity summaries 2023, Mineral Commodity Summaries. Reston, VA, p. 210.
Valenzano, L., Civalleri, B., Chavan, S., Palomino, G.T., Areán, C.O., Bordiga, S., 2010. Computational and Experimental Studies on the Adsorption of CO, N_2, and CO_2 on Mg-MOF-74. The Journal of Physical Chemistry C 114(25), 11185-11191.
Volkov, A., Vasilevsky, V., Bazhenov, S., Volkov, V., Rieder, A., Unterberger, S., Schallert, B., 2014. Reclaiming of Monoethanolamine (MEA) Used in Post-Combustion CO_2-capture with Electrodialysis. Energy Procedia 51, 148-153.
Weir, H., Sanchez-Fernandez, E., Charalambous, C., Ros, J., Monteiro, J.G.M.-S., Skylogianni, E., Wiechers, G., Moser, P., van der Spek, M., Garcia, S., 2023. Impact of high capture rates and solvent and emission management strategies on the costs of full-scale post-combustion CO_2 capture plants using long-term pilot plant data. International Journal of Greenhouse Gas Control 126, 103914.
World Resources Institute, 2014. Greenhouse Gas Protocol - Policy and Action Standard.
Xia, W., Lau, S.K., Yong, W.F., 2022. Comparative life cycle assessment on zeolitic imidazolate framework-8 (ZIF-8) production for CO_2 capture. Journal of Cleaner Production 370, 133354.
Yadav, S., Mondal, S.S., 2022. A review on the progress and prospects of oxy-fuel carbon capture and sequestration (CCS) technology. Fuel 308, 122057.
Yang, B., Wei, Y.-M., Hou, Y., Li, H., Wang, P., 2019. Life cycle environmental impact assessment of fuel mix-based biomass co-firing plants with CO_2 capture and storage. Applied Energy 252, 113483.

Appendix

Appendix A *Estimates for coal-fired electricity generation in the United States from 2020 to 2050 (Unit: TWh).*

	2020	**2025**	**2030**	**2035**	**2040**	**2045**	**2050**
Subcritical	727	618	241	185	122	66	0
Subcritical CC	0	15	28	45	60	70	73
Supercritical	46	0	0	0	0	0	0
Supercritical CC	0	122	76	75	64	57	49
Ultra-supercritical CC	0	0	0	35	55	86	121
Total:	773	755	345	340	300	279	243

Appendix B *Technical parameters of three types of coal-fired power plants without carbon capture and with MEA-based or MOF-based carbon capture (Ansolabehere et al., 2007; Sathre and Masanet, 2013).*

	Subcritical			**Supercritical**			**Ultra-supercritical**		
	No capture	**MEA capture**	**MOF capture**	**No capture**	**MEA capture**	**MOF capture**	**No capture**	**MEA capture**	**MOF capture**
Heat rate (MJ/MWh)	10498	14349	13353	9359	12344	11574	8314	10551	10007
--Turbines	10498	10498	10498	9359	9359	9359	8314	8314	8314
--Capture media regeneration	0	2093	1219	0	1623	938	0	1216	725
--CO_2 compression	0	1465	1363	0	1136	1065	0	851	807
--Auxiliary capture loads	0	293	273	0	227	213	0	170	161
Coal feed (t/MWh)	0.41	0.57	0.53	0.37	0.49	0.46	0.33	0.42	0.39
CO_2 emitted (t/MWh)	0.93	0.13	0.12	0.83	0.11	0.1	0.74	0.09	0.09
CO_2 captured (t/MWh)	0	1.15	1.07	0	0.98	0.92	0	0.84	0.8